CHINESE JOURNAL OF MECHANICAL ENGINEERING
Vol. 27, No. 4, 2014

DOI: 10.3901/CJME.2014.0515.095, available online at www.springerlink.com; www.cjmenet.com; www.cjmenet.com.cn

Influence of Surrounding Structures upon the Aerodynamic and Acoustic Performance of the Outdoor Unit of a Split Air-Conditioner

WU Chengjun[1, *], LIU Jiang[1], and PAN Jie[2]

1 *School of Mechanical Engineering, Xi'an Jiaotong University, Xi'an 710049, China*
2 *School of Mechanical and Chemical Engineering, The University of Western Australia,Crawley, WA 6009, Australia*

Received September 26, 2013; revised May 14, 2014; accepted May 15, 2014

Abstract: DC-inverter split air-conditioner is widely used in Chinese homes as a result of its high-efficiency and energy-saving. Recently, the researches on its outdoor unit have focused on the influence of surrounding structures upon the aerodynamic and acoustic performance, however they are only limited to the influence of a few parameters on the performance, and practical design of the unit requires more detailed parametric analysis. Three-dimensional computational fluid dynamics(CFD) and computational aerodynamic acoustics(CAA) simulation based on FLUENT solver is used to study the influence of surrounding structures upon the aforementioned properties of the unit. The flow rate and sound pressure level are predicted for different rotating speed, and agree well with the experimental results. The parametric influence of three main surrounding structures(i.e. the heat sink, the bell-mouth type shroud and the outlet grille) upon the aerodynamic performance of the unit is analyzed thoroughly. The results demonstrate that the tip vortex plays a major role in the flow fields near the blade tip and has a great effect on the flow field of the unit. The inlet ring's size and throat's depth of the bell-mouth type shroud, and the through-flow area and configuration of upwind and downwind sections of the outlet grille are the most important factors that affect the aerodynamic performance of the unit. Furthermore, two improved schemes against the existing prototype of the unit are developed, which both can significantly increase the flow rate more than 6 %(i.e. 100 $m^3 \cdot h^{-1}$) at given rotating speeds. The inevitable increase of flow noise level when flow rate is increased and the advantage of keeping a lower rotating speed are also discussed. The presented work could be a useful guideline in designing the aerodynamic and acoustic performance of the split air-conditioner in engineering practice.

Keywords: DC-inverter split air-conditioner, outdoor unit, surrounding structure, computational fluid dynamics(CFD), computational aerodynamic acoustics(CAA), simulation, improved design

1 Introduction

The DC-inverter split air-conditioner is regarded as an alternative of the fixed-speed air-conditioner in the near future due to its high-efficiency and energy-saving. The development of low-noise emission and energy-saving air-conditioners has always been the important goals of practical design and manufacturing[1]. Fig. 1 shows pictures of the outdoor unit of a widely used split air-conditioner with DC inverter, which is structurally more complicated than its indoor counterpart[1].

Over the past decade, many studies[1–20] have been devoted to achieve these design goals. The time accurate turbulence simulation such as large eddy simulation (LES)[2–11] and unsteady Reynolds-averaged Navier-Stokes (URANS) method[1, 11–20] were used to compute the space-time history of the three-dimensional flow field of the outdoor unit. Then the generalized Lighthill equation and its extended forms, such as Ffowcs Williams-Hawkings (FW-H) equation, Curle equation, and Lowson formulation, were applied to predict the corresponding sound field of the unit.

It is worth mentioning that in addition to the axial-flow fan, some surrounding structures, such as the bell-mouth type shroud, the outlet grille and the electric motor bracket, would also significantly affect the aerodynamic and acoustic performance of the unit. In this regard, recent researches have achieved some valuable results, which will be briefly summarized as follows. In order to determine the influence of the upstream flow path on the acoustic and aerodynamic behavior of axial-flow fans, MAALOUM, et al[14], analyzed the effect of a contoured duct at the inlet of an axial-flow fan on the flow noise generation. They found a strong involvement of the upstream turbulence level in the generation of the noise, and in particular, of the broadband noise. By using STAR-CD, HU, et al[15–16], investigated the influence of air outlet louver and deflecting ring on the noise generated by the outdoor unit. Their study demonstrated that the circular shaped air outlet louver

* Corresponding author. E-mail: cjwu@mail.xjtu.edu.cn
Supported by Program for Changjiang Scholars and Innovative Research Team in University, Ministry of Education of China(PCSIRT)

yielded a lower noise generation, and the deflecting ring with double contoured duct could improve the aerodynamic performance and reduce the noise generated by the outdoor unit. TIAN, et al[17], studied the aerodynamic and acoustic performance of the outdoor unit with two different types of grille. Their results indicated that the grille affected the flow rate and increased the level of broadband noise of the outdoor unit. WEI, et al[18], examined the flow performance of an outdoor unit by changing the radius of fan shroud, depth and other surrounding structures. They concluded that the inlet radius of the fan shroud and the fan guard grille were most significant factors, and the flow field improvements were achieved by minimizing the flow recirculation and separation.

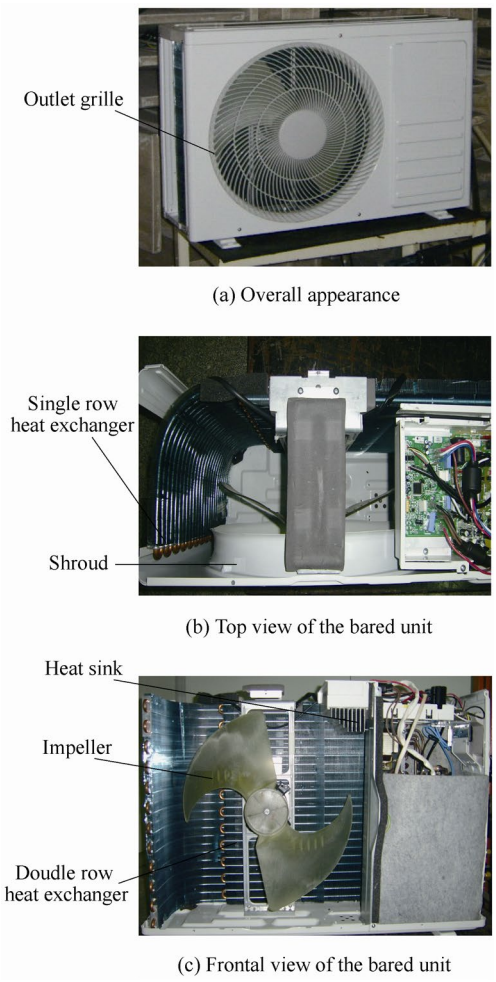

Fig. 1. Present outdoor unit of a DC-inverter split air-conditioner

Although all these previous studies are on the influence of different surrounding structures upon the aerodynamic and acoustic performance of the outdoor unit, they focused on some specific parameters of the unit. Taking the bell-mouth type shroud as an example, its geometrical parameters includes the radius and central angle of the inlet ring, the diameter and depth of the throat, and the divergence angle and depth of the outlet ring. The diameter and depth of the bell mouth described in Refs. [16, 18] are only two of the many parameters of the shroud that may affect the flow and the flow-induced noise. Moreover, the previous studies on the outlet grille are limited to the simple layouts of the grille(rectangular or circular type). As a matter of fact, the through-flow area and configuration of upstream and downstream sides of the grille are the more important influencing factors on the aerodynamic performance of the unit. Heat sink of the DC inverter box in the outdoor unit may also affect the aerodynamic performance of the unit. However, this effect has not been systematically investigated in the existing literatures. Hence, there is a need for a more detailed study on the influence of these surrounding structures upon the aerodynamic performance of the outdoor unit.

In this paper, a study of the influence of above surrounding structures upon the aerodynamic and acoustic properties of an outdoor unit of a DC-inverter split air-conditioner are conducted using the well-known CFD solver FLUENT. The study consists of numerical predictions, experimental verification and parametric analysis. Sections 2 and 3 respectively detail the CFD and CAA simulations including the meshes of computational model and the selection of algorithm. In Section 4, the parametric analysis is undertaken to illustrate the influence of heat sink, bell-mouth type shroud and outlet grille on the aerodynamic performance of the unit, and to describe the development of improved schemes for the existing prototype unit based on the aforementioned results. Section 5 concludes the paper. It is worthwhile to note that increasing flow rate is often accompanied by the increase of flow noise. However, how to effectively increase the flow rate of the unit and without too much increase in flow noise level has been a challenging question to the air-conditioner manufacturers. Equally important question is how to maintain the same flow rate with decreased rotating speed. The former focuses on the aerodynamic performance, while the later concentrates on the energy efficiency and reduction of wear. Part of the effort of this paper aims at illustrating the first question. The results of analysis also indirectly demonstrate that the solution of the second question is feasible.

2 CFD Simulation

2.1 Meshing of the computational model

In this section, a pre-processing software GAMBIT is utilized to mesh the computational model of the unit prior to CFD simulation. In order to set the boundary conditions so that they agree well with the practical situation, the frontal inlet, the side inlet and the outlet of the unit are all extended 2600 mm firstly. As shown in Fig. 2, tetrahedron meshes are adopted, and the computational domain is divided into two zones, a rotating zone including impeller, and a stationary zone. A sliding mesh

technique[20] is applied at the interface in order to allow the unsteady interactions of the fluids between two zones. The overall numbers of cells are 1 377 455(without grille) and 3 126 958(with grille), respectively, which could meet the convergence requirement by cell independence verification. The number of cells in the rotating zone is 332978 and that of the stationary zone(including duct system, inlet and outlet extensions) are 1 044 477(without grille) and 2 793 980(with grille) respectively.

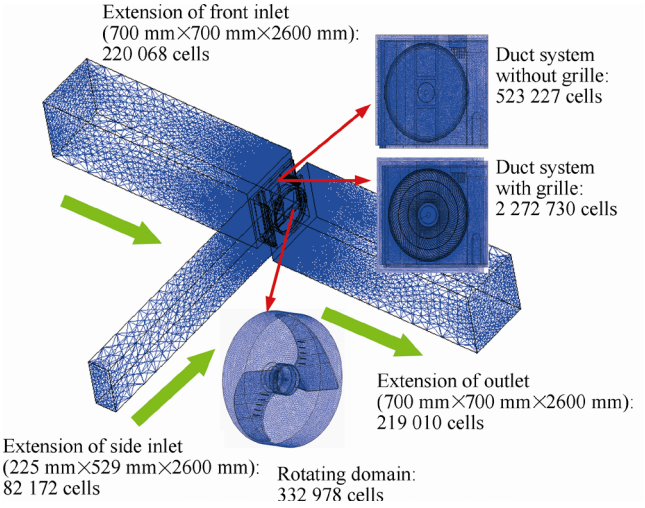

Fig. 2. Meshes of the computational model of the unit

2.2 Boundary conditions and modeling of heat exchanger

Since the axial-flow fan of the outdoor unit often operate at a low rotating speed within 720–870 r/min, the flow inside the unit is assumed to be incompressible, and the influences of radiation heat and other properties on the flow field are neglected[8, 15–16, 18]. The atmospheric pressure is taken as the pressure boundary conditions at the inlet and outlet of the flow due to the fact that the outlet volume flow rate is chosen for evaluating the aerodynamic performance of the unit.

It is worth mentioning that since there is a significant resistance towards the inlet flow of the outdoor unit due to the presence of heat exchanger. Usually, it is modeled as the porous media in FLUENT, where the characteristic relation of the flow can be written as[21]

$$\Delta p = t_{\mathrm{ex}}\left(\frac{\mu}{\alpha}v_i + C_2\frac{1}{2}\rho|v|v_i\right), \tag{1}$$

where Δp and t_{ex} denote the static pressure drop across heat exchanger and the thickness of heat exchanger, respectively. v_i is the velocity of inlet flow, $|v|$ is the magnitude of the velocity, and ρ is the density of air. $1/\alpha$ and C_2 represent the viscous damping factor and the inertial damping factor, respectively, which can be obtained from the measured static pressure drop Δp across the two terminals of the heat exchanger as functions of the inlet velocity v_i.

As shown in Fig. 1, where the heat exchanger of the present unit has a combination profile of single-row and double-row, thus they are measured respectively in an air chamber of enthalpy difference laboratory. Fig. 3 shows the static pressure drops versus different inlet velocities for the single-row and double-row heat exchangers respectively, and the corresponding curve-fitting results. Inserting these two fitted formulae into Eq. (1), one can obtain C_2=213.259 m^{-1} and $1/\alpha$=9.937 6×10^6 m^{-2} for single-row heat exchanger, and C_2=143.201 m^{-1} and $1/\alpha$=9.485 2×10^6 m^{-2} for double-row heat exchanger, respectively.

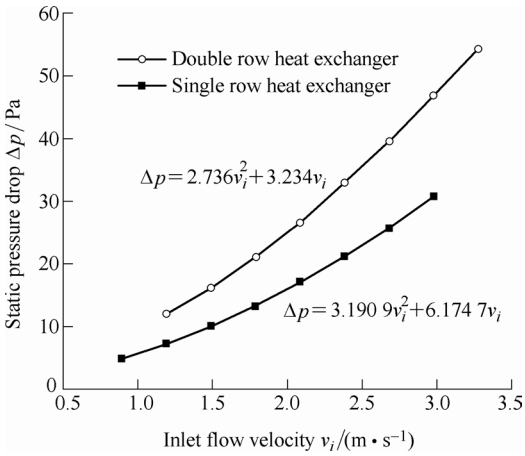

Fig. 3. Static pressure drop versus inlet velocity for different heat exchanger

2.3 Three dimensional calculations

It is well known that the three dimensional incompressible Navier-Stokes equations in a moving coordinate can be written as[20]

$$\frac{\partial \boldsymbol{Q}}{\partial t}+\frac{\partial \boldsymbol{F}}{\partial x}+\frac{\partial \boldsymbol{G}}{\partial y}+\frac{\partial \boldsymbol{H}}{\partial z}=\frac{1}{Re}\left(\frac{\partial \boldsymbol{F}_v}{\partial x}+\frac{\partial \boldsymbol{G}_v}{\partial y}+\frac{\partial \boldsymbol{H}_v}{\partial z}\right), \tag{2}$$

where

$$\boldsymbol{Q}=\begin{pmatrix}0\\u\\v\\w\end{pmatrix},\ \boldsymbol{F}=\begin{pmatrix}u\\u(u-w_x)+p\\v(u-w_x)\\w(u-w_x)\end{pmatrix},$$
$$\boldsymbol{G}=\begin{pmatrix}v\\u(v-w_y)\\v(v-w_y)+p\\w(v-w_y)\end{pmatrix},\ \boldsymbol{H}=\begin{pmatrix}w\\u(w-w_z)\\v(w-w_z)\\w(w-w_z)+p\end{pmatrix}, \tag{3}$$

$$\boldsymbol{F}_{\mathrm{v}}=\boldsymbol{I}_{\mathrm{m}}\frac{\partial \boldsymbol{Q}}{\partial x},\ \boldsymbol{G}_{\mathrm{v}}=\boldsymbol{I}_{\mathrm{m}}\frac{\partial \boldsymbol{Q}}{\partial y},$$
$$\boldsymbol{H}_{\mathrm{v}}=\boldsymbol{I}_{\mathrm{m}}\frac{\partial \boldsymbol{Q}}{\partial z},\ \boldsymbol{I}_{\mathrm{m}}=\begin{pmatrix}0&0&0&0\\0&1&0&0\\0&0&1&0\\0&0&0&1\end{pmatrix}. \tag{4}$$

In the above, u, v and w represent the velocity at x, y and z-axis direction, respectively, (w_x, w_y, w_z) is a moving velocity vector, the subscript v denotes the viscous terms, and Re is the Reynolds number.

In this paper, the three-dimensional URANS simulations of the outdoor unit with and without grille have been carried out by the CFD solver FLUENT(version 6.3). The stand k-ε turbulence model is used to model the effects of turbulence on the flow field. The time-dependent term "scheme" is of second order, implicit. The pressure-velocity coupling is calculated through SIMPLE(Semi-Implicit Method for Pressure Linked Equations) algorithm. The second-order upwind method is used in the discretization of momentum, turbulent kinetic energy and turbulent dissipation rate. The rotating speed of the fan is set 720 r/min, and the time step of the unsteady calculations is chosen as 7.5×10^{-4} s in order to get adequate time resolution for the dynamic analysis.

In order to verify the accuracy of three-dimensional computations, the flow rates of the unit corresponding to the fan's rotating speed at 720, 810, and 870 r/min are presented respectively, and compared with the experimental results in Fig. 4. It is shown that with the increase of the rotating speed, the value of flow rate increases linearly, which is consistent with the observation in TIAN, et al[17]. The flow rate of the unit without grille is bigger(about 210–240 $m^3 \cdot h^{-1}$) than that of the unit with grille for the same rotating speeds. The comparison shows that the flow rate of the unit could be predicted very accurately(with a maximum error within 3%) by using the appropriate computational algorithm and meshing if the drag coefficients of the heat exchanger are selected correctly.

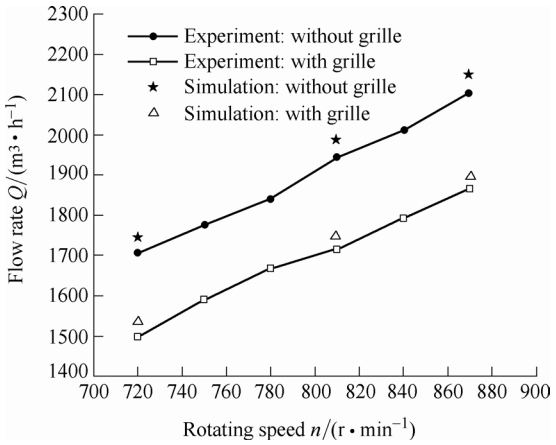

Fig. 4. Flow rate versus rotating speed of the unit with and without grille

3 CAA Simulation

As the dominant noise source of the outdoor unit is the aerodynamic noise originated from the operation of the axial-flow fan, the prediction of mechanical noise and of the noise generated from the compressor-accumulator assembly is of secondary importance and thus not discussed in this paper.

In this section, the LES simulation is firstly adopted to calculate the flow field of the unit instead of the previous URANS simulation due to the fact that the former has an advantage for predicting the broadband noise generated from the outdoor unit. The Smagorinsky-Lilly model is used as sub-grid scale model, and the bounded central differencing scheme is utilized in the discretization for the corresponding convection and diffusion terms. The time step of the unsteady calculations is chosen as 1×10^{-4} s. Other system parameters not mentioned herein are consistent with the previous URANS simulation described in section 2.3. The aerodynamic noise is calculated by the FW−H model of FLUENT solver based on the fluctuating pressure on the blade surface calculated by LES. The frequency band selected for analysis is 0–5000 Hz with a 3 Hz resolution. The effects of unit casing and inter blade acoustic interference such as reflection, diffraction, and scattering are neglected in the present CAA calculations because the acoustic wavelength(i.e. 12.7 m for 810 r/min) of BPF1(i.e. 27 Hz for 810 r/min) noise of the axial-flow fan is much longer than the fan's characteristic dimensions.

In Table 1, the measured overall sound pressure level ($OASPL$) and sound pressure level($SPL_{0\text{-}5kHz}$) within the frequency range of interest(0–5000 Hz) are listed and compared with the predicted $SPL_{0\text{-}5kHz}$. The measured $SPL_{0\text{-}5kHz}$ is very close to the measured $OASPL$(within 0.11 dBA), which means that the majority of the acoustic energy is within 0–5000 Hz at the selected testing speeds(810, 840 or 870 r/min). It is also noted that the predicted $SPL_{0\text{-}5kHz}$ agrees well with the measured one at the three rotating speeds with a maximum error of 1.61 dBA.

Table 1. Measured and predicted sound pressure level of the unit with grille at various rotating speeds

Rotating speed $n/(r \cdot min^{-1})$	Measured sound pressure level $OASPL$/dBA	Measured sound pressure level $SPL_{0\text{-}5kHz}$/dBA	Predicted sound pressure level $SPL_{0\text{-}5kHz}$/dBA
810	51.47	51.36	50.79
840	52.67	52.57	51.65
870	53.67	53.58	51.97

For convenience, $SPL_{0\text{-}5kHz}$ is chosen for evaluating the acoustic performance in the subsequent studies.

4 Parametric Analysis and Improved Design

As shown in Fig. 1, the duct system(with exception of the compressor-accumulator assembly) of the present outdoor unit is more complicated than a single axial-flow fan. It consists of not only the axial-flow fan but also the heat exchanger and some necessary surrounding structures, i.e. the outlet grille, the bell-mouth type shroud, the electric

motor bracket and the specific heat sink used to dissipate the heat from the DC-inverter box in the unit. It is demonstrated that these surrounding structures can change either the flow field or noise level to a certain extent of the outdoor unit. Consequently, it is of great significance for analyzing the influence of these structures' parameters or layouts upon the properties of the unit. In the subsequent analysis, these surrounding structures except the electric motor bracket are taken into account due to the corresponding incomplete studies in the existing literatures. It is worth emphasizing that since the main objective of this practical work is to increase the flow rate as far as possible, only the aerodynamic property is considered and the flow rate is chosen as the evaluation indicator for saving computation costs.

Here, in order to evaluate the flow rate of the existing unit (prototype) and use it as a reference for improving the prototype, the effects of layout or parametric change of the heat sink, the bell-mouth type shroud and the outlet grille upon the values of flow rate are numerically analyzed. Note that the three-dimensional computations are applied in the subsequent studies all the time, and the corresponding algorithm and parameters are consistent with the aforementioned sections.

4.1 Influence of heat sink

The heat sink is a key component structure that is mainly used to dissipate the heat emitted from the DC-inverter box of the outdoor unit. A study of the fins' layout of heat sink and its influence on the aerodynamic performance is essential to the practical design. In the proceeding studies, two different layout of heat sink(Types A and B, see Fig. 5) are considered. For the further understanding of the flow characteristics around these two heat sinks, the corresponding velocity vector distributions located at four different longitudinal(axial) or transverse(radial) sections (defined in Fig. 5) are visualized in Figs. 6 and 7, respectively. The aerodynamic parameters are compared in Table 2.

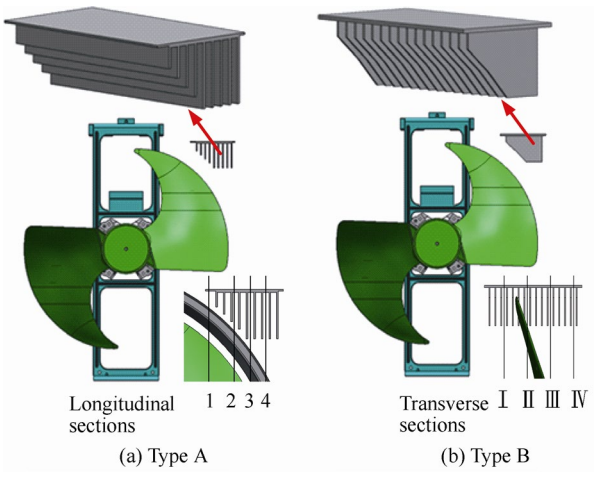

Fig. 5. Heat sinks for DC-inverter box

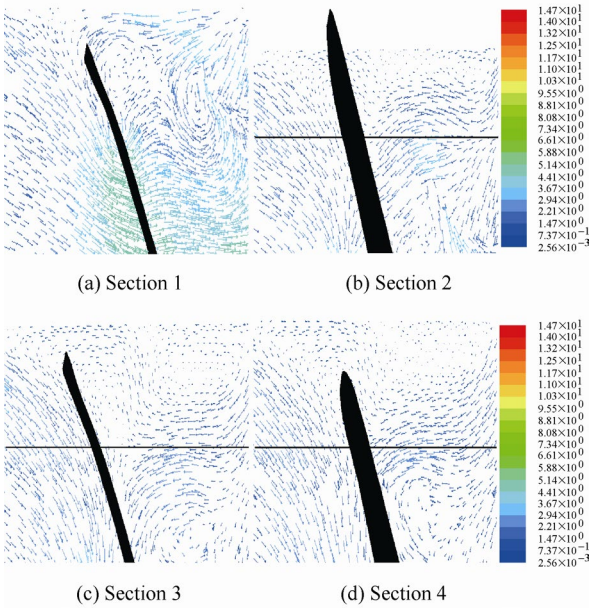

Fig. 6. Velocity vector at longitudinal section of the unit with Type A sink
(The black lines denote the lower edges of the adjacent fins)

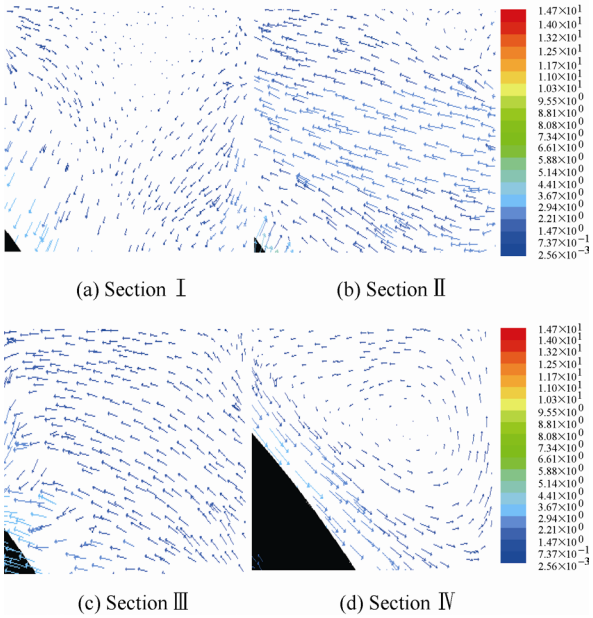

Fig. 7. Velocity vector at transverse section of the unit with Type B sink

Table 2. Aerodynamic parameter for different heat sink of the unit without grille (800 r/min)

Case	Flow rate $Q/(m^3 \cdot h^{-1})$	Maximum pressure P_{max}/Pa	Maximum velocity $v_{max}/(m \cdot s^{-1})$
Without sink	1917	55.1	17.5
Type A sink	1916	55.9	17.5
Type B sink	1915	55.1	17.5

It can be observed that influenced by the blade, the main flow domain(MFD) that can be utilized for dissipating the heat of the sink is located between the suction surface of the blade tip and the bell-mouth type shroud, where the mostly circumferential moving flow can be found. For Type A sink(axial layout, corresponding to the prototype), the

fluidity of the flow at MFD is significantly poor except at the lower edge of fins. It means that the fins layout of Type A sink is not capable of removing the heat sufficiently. Alternatively, Type B sink (radial layout) can effectively make use of the circumferential moving flow at MFD for removing the heat. Moreover, one can see from Table 2 that both heat sinks have little influence upon the aerodynamic performance as the values of the presented flow parameters with and without the sinks remain almost unchanged. As a result, based on an overall consideration of heat emission and aerodynamic performance, we recommend Type B sink for the practical design of product.

4.2 Influence of bell-mouth type shroud

The bell-mouth type shroud, also known as deflecting ring[16] or nozzle[18], has always been an important surrounding structure that can prevent the flow out of the axial-flow fan from diffusing. As shown in Fig. 8, the shroud of the unit has a rounded inlet ring(to decrease the turbulent noise) and a chamfered outlet ring(to avoid Coanda effect, and create a more axially directed flow[18]). In order to evaluate the influence of the shroud upon the flow rate of the unit, several geometric parameters (i.e. the radius R and central angle θ of the inlet ring, the diameter D_t and depth H_1 of the throat, and the divergence angle α and depth H_2 of the outlet ring) that can fully characterize the shroud are taken into consideration. For this investigation, the rotating speed of the unit is set 720 r/min, and the outlet grille is removed.

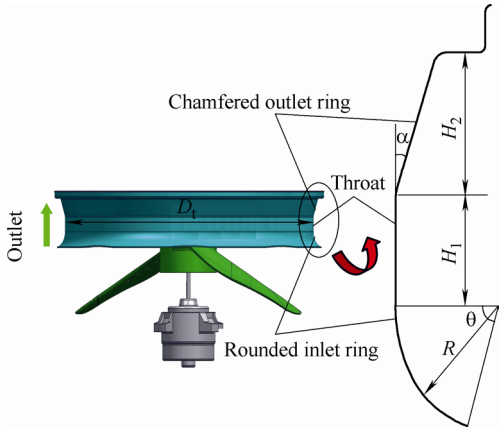

Fig. 8. Bell-mouth type shroud of the unit

The corresponding parametric analysis is carried out and the flow rates versus different parameters are shown in Figs. 9(a)–(f), respectively. It can be seen that when the characteristic parameters of the shroud change, the flow field of the outdoor unit will be changed, resulting different outlet flow rate. The flow rate Q increases with the increase of R, θ and H_1, while decreases with the increase of D_t, H_2 and α.

To compare the efficiency of the change of the parameters on the flow rate, an one-order sensitivity dQ/dx (x denotes different characteristic parameters of the shroud), and a ratio $\Delta Q_m/Q_p$(describes the maximal increment of the flow rate ΔQ_m with respect to the flow rate Q_p=1745 $m^3 \cdot h^{-1}$ of prototype without outlet grille at 720 r/min) are introduced. It is clear that the larger of magnitude of these two indicators represents the stronger effect on the flow rate of the corresponding parameter change.

To rank the relative influence to the flow rate by the parameter changes, a more intuitively bar-graph derived from Fig. 9 is shown in Fig. 10.

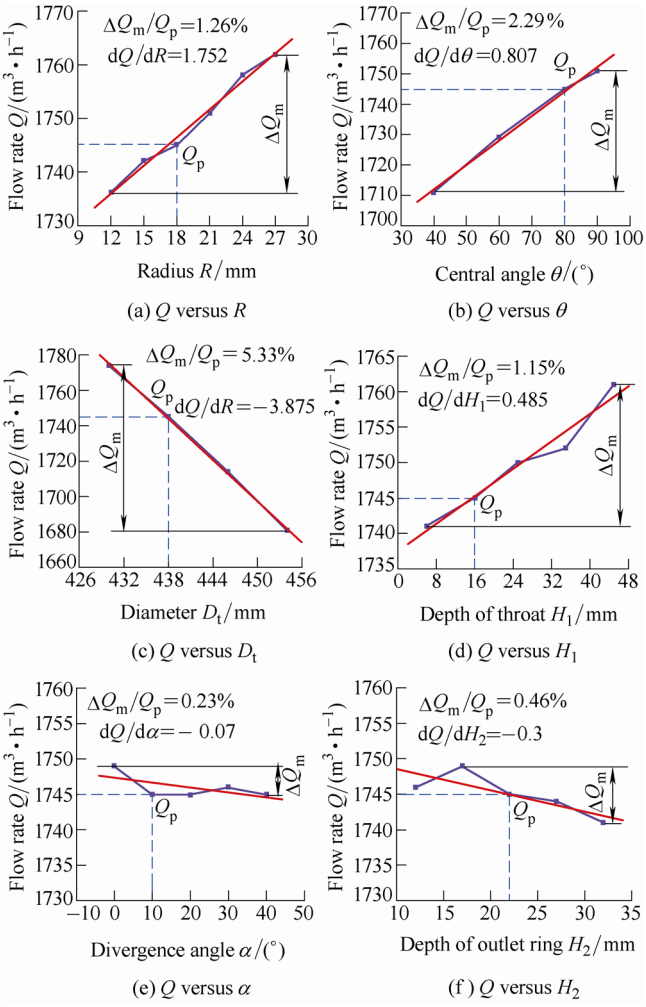

Fig. 9. Flow rate versus characteristic parameter of the shroud

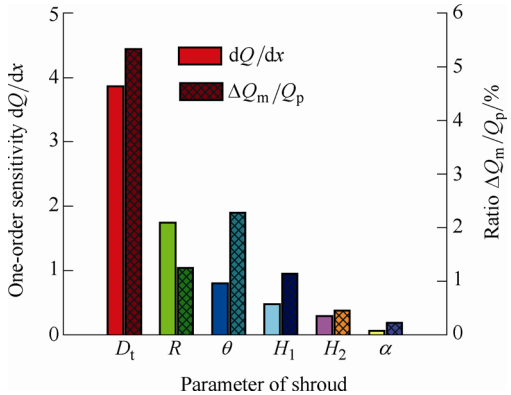

Fig. 10. Values of dQ/dx and $\Delta Q_m/Q_p$ for different characteristic parameter of the shroud

The following results can be obtained:

(1) For dQ/dx, the ranking is D_t (3.875) > R (1.752) > θ (0.807) > H_1 (0.485).

(2) For $\Delta Q/Q_p$, the ranking is D_t (5.33%) > θ (2.29%) > R (1.26%) > H_1 (1.15%).

(3) The chamfered outlet ring(described by H_1 and α) has little influence upon the flow rate of the unit except for a good air-throw direction.

These results indicate that four parameters of the shroud (i.e. D_t, R, θ and H_1) are the main factors that effectively affect the flow rate of the unit. The interaction with unsteady flow at the blade tip is very sensitive to D_t. Further decrease of D_t may result in a higher noise penalty in the practical design. Thus, as mentioned in Refs. [16, 18], the main parameters that can improve the flow rate practically are the size(radius or central angle) of inlet ring and the depth of throat. It was suggested that the size of inlet ring and the depth of throat are the most important factors that can affect the aerodynamic performance of the outdoor unit. Therefore increasing them to some appropriate values can effectively improve the flow rate of the unit.

4.3 Influence of outlet grille

The outlet grille is also an indispensable structure of the outdoor unit that has always been the concern at the design phase. Previous studies[15, 17–18] show that the flow field of the unit with the outlet grille attached is more complex than that of the unit without the grille. The discharge flow of the axial-flow fan and its interaction with outlet grille affect the aerodynamic performance of the unit, as well as the radiated aerodynamic noise. Fig. 11 shows the measured relationship between Q and $OASPL$ of the unit with and without grille respectively. Note that the flow rate is closely related to the aerodynamic noise of the unit. The value of $OASPL$ increases linearly with the increase of the flow rate Q. At the same flow rate, the outlet grille increases the $OASPL$ of the outdoor unit for more than 3 dBA. As a result, there is a need for more indepth research into the influence of the outlet grille upon the aerodynamic performance of the unit. Here, eight different configurations of outlet grille are examined, as shown in Fig. 12, and the corresponding calculation results of the flow rate in comparison with that of the prototype (see Fig. 1(a), a protruding radial-type grille like Fig. 12(f)) are listed in Table 3.

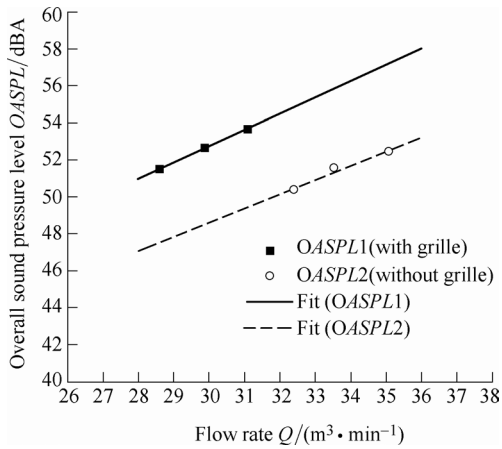

Fig. 11. Overall sound pressure level versus flow rate of the unit with and without grille

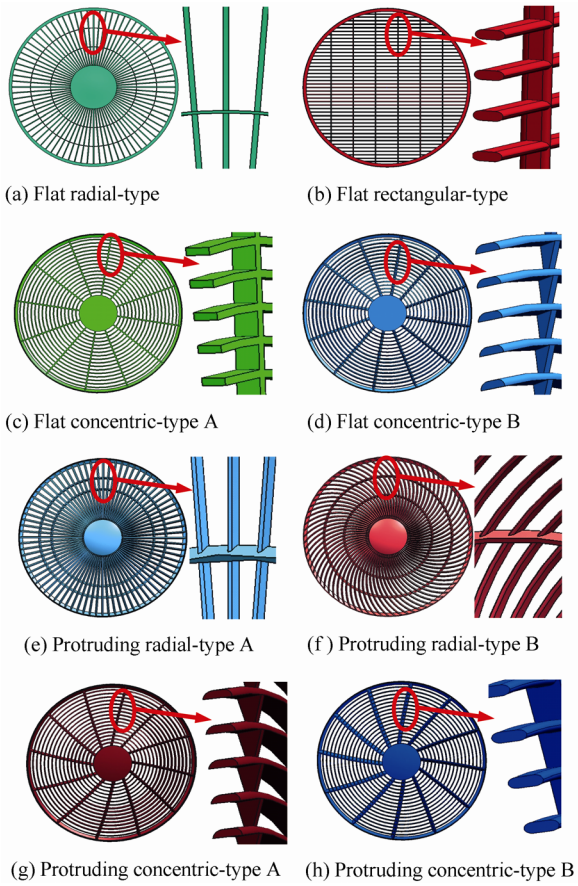

Fig. 12. Various configurations of the outlet grille

Table 3. Flow rate of the unit with different type of outlet grille(720 r/min)

Case	Through-flow area A_{th}/mm^2	Flow rate Q/(m^3 • h^{-1})	Increment ΔQ/(m^3 • h^{-1})	Ratio $\Delta Q/Q_p$
Prototype(protruding radial-type)	105 230	1539 (Q_p)	–	–
Flat radial-type	–	1506	–33	–2.14 %
Flat retangular -type	114 710	1615	76	4.94 %
Flat concentric-type A	111 890	1444	–95	–6.34 %
Flat concentric-type B	111 890	1563	24	1.56 %
Protruding radial-type A	–	1588	49	3.18 %
Protruding radial-type B	–	1560	21	1.36 %
Protruding concentric-type A	111 890	1596	57	3.70 %
Protruding concentric-type B	111 890	1613	74	4.81 %

It is worth noting from Table 3 that the flat rectangular-type(see Fig. 12(b)) and the protruding concentric-type B (see Fig. 12(h)) are the two most effective configurations of grille that can increase 76 m^3 • h^{-1} and 74 m^3 • h^{-1} of the flow rate respectively, as opposed to the prototype one. This may due to the fact that the through-flow areas A_{th} for these two grilles(114 710 mm^2 and 111 890 mm^2, respective-

ly) are bigger than that of the prototype grille(105 230 mm^2). However, large area does not mean that the corresponding flow rate is bound to become larger. For example, the values of A_{th} for four concentric-type grilles(all equal 111 890 mm^2) in Table 3 are all bigger than that of the prototype grille, however, the flow rate Q are not all bigger than the latter. Obviously, the flow rate of the unit with the flat concentric-type grille is lower 95 m^3 • h^{-1} than the prototype even though it has a bigger value of A_{th}. When changing it as a form of protruding configuration, an increment of 14 m^3 • h^{-1} can be achieved. It will be seen from this that the through-flow area is not the only factor that affect the flow rate of the unit, which also depends on the appearance of the grille, i.e. the configuration of upwind side and downwind side of the grille. This can be demonstrated by the fact that the flow rate of the unit with the protruding radial-type B is larger 21 m^3 • h^{-1} than that of the prototype, which have the same appearance as the former only except the different configuration of the upwind and downwind sections. Moreover, the flat concentric-type B grille's flow rate also exceeds 100 m^3 • h^{-1} with respect to that of the similar type A grille on this account(see Figs. 12(c)–(d)).

Similar results can also be found when a couple of other grilles(see Figs. 12(g)–(h) for the protruding concentric-type A and B) are selected. These observations indicate that the configuration of upwind and downwind sides of the outlet grille is also an important factor which can affect the aerodynamic performance of the outdoor unit.

4.4 Improved design and assessment

The aforementioned results from the parametric analysis show that there is a room for improving the aerodynamic performance of the prototype unit by using the new design of the bell-mouth type shroud and the outlet grille. In the subsequent analysis, a new shroud(whose radius of the inlet ring is changed from 18 mm to 27 mm, and the depth of throat is extended from 16 mm to 40 mm) is firstly considered. Then, two improvement schemes(Improvements I and II) are developed in a hope that a feasible design can significantly increase the flow rate without significantly increasing the noise level. These two schemes are developed respectively from a combination of above new shroud and the two best outlet grilles(i.e. the protruding concentric-type B and the flat rectangular-type, as shown in Fig. 12(h) and Fig. 12(b))already described in the previous section.

It is worth noting that the present improved designs are fully dependent on the previous results of parametric analysis with the main objective of increasing the flow rate of the unit. Increased flow rate allows significant improvement of the aerodynamic efficiency, while maintaining the unit's operation at a relatively lower rotating speed with identical flow rate directly implicates the energy efficiency and reduction of wear. However, increase of noise level with increased flow rate is inevitable. The task of this analysis is to find out how much flow noise will increase with increased flow rate, and how much reduction of rotating speed at the same flow rate level can be achieved. The flow rate, rotating speed and sound pressure level below 5000 Hz of the unit before and after improvements are all listed in Table 4.

Table 4. Flow rate and sound pressure of the unit before and after improvement

Case	720 r/min		810 r/min	
	Flow rate Q/(m^3•h^{-1})	Sound pressure $SPL_{0\text{-}5kHz}$/dBA	Flow rate Q/(m^3•h^{-1})	Sound pressure $SPL_{0\text{-}5kHz}$/dBA
Prototype	1539	49.12	1755	50.79
Improvement I	1644 (+105)	50.78 (+1.66)	1875 (+120)	53.13 (+2.34)
Improvement II	1649 (+110)	50.80 (+1.68)	1883 (+128)	53.10 (+2.31)

Values with positive sign "+" in parenthesis denote the corresponding increment in comparison with the prototype, respectively.

The corresponding velocity contour in Fig. 13 is also presented for further illustration of increased flow rate. It can be clearly shown that at the downstream of the fan, the flow velocities of the two improved schemes are larger than that of the prototype.

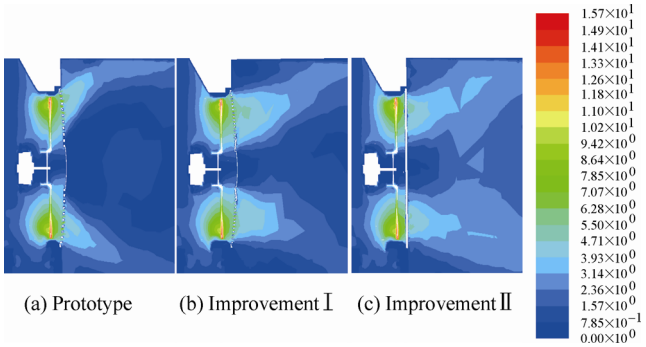

(a) Prototype (b) Improvement Ⅰ (c) Improvement Ⅱ

Fig. 13. Velocity contour for the unit before and after improvements

In summary, we observe the following three features:

(1) Compared with that of the original prototype, more than 6%(i.e.100 m^3 • h^{-1}) of the flow rates is achieved by the improved designs.

(2) Each comparison is against the same rotating speeds (720 r/min and 810 r/min). This means that the improved designs are capable of delivering increased flow rates at the same rotating speed.

(3) There is a corresponding noise level increase that is approximately proportional to the increase of the flow rate.

The above summary is further detailed in Fig. 14, where the increase in sound pressure level $\Delta SPL_{0\text{-}5kHz}$ and the increase in rotating speed $\triangle n$ between the improved designs and the original prototype are respectively plotted against the flow rate Q. It becomes clear that above certain critical flow rates(1297.5 m^3 • h^{-1} for Improvement I, and 1252.1 m^3 • h^{-1} for Improvement II) both improved designs are capable of using lower rotating speed($\triangle n < 0$) to

deliver the required flow rate. In another words, with the same rotating speed, the improved designs can produced higher flow rate than that the original prototype could. However in this range of flow rate, we observe an increased sound pressure level at the rate of 0.0024 dBA/(m^3 • h^{-1})(for Improvement I) and 0.0021 dBA/(m^3 • h^{-1})(for Improvement II).

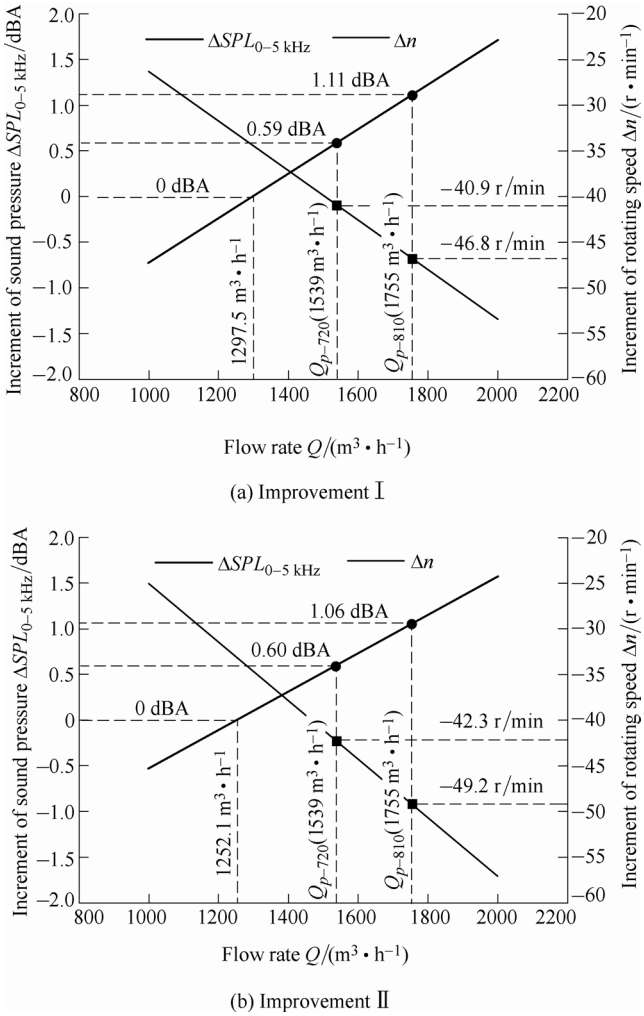

Fig. 14. Increment of sound pressure level and rotating speed versus flow rate for improved schemes

Below the critical flow rate, the improved designs achieve the same flow rate with both decreased rotating speeds and decreased noise emission. However, practical units often operate at relatively higher flow rate.

Although flow noise is in principle proportional to flow rate and the improved designs gain the advantage of having reduced rotation speed to achieve the same flow rate, further work of reducing the rate of noise increase with respect to the flow rate is required.

5 Conclusions

(1) The aerodynamic and acoustic performance of an outdoor unit of a domestic DC-inverter split air-conditioner is presented. The unsteady three-dimensional CFD and CAA simulations for the unit have been carried out by using the commercial flow solver FLUENT.

(2) The numerical predictions on the flow rate and sound pressure level of the unit are presented and verified by the experimental testing, well agreement between the prediction results and experimental results show that the proposed simulation by FLUENT solver is correct.

(3) The parametric influence of three main surrounding structures (i.e. the heat sink, the bell-mouth type shroud and the outlet grille) upon the aerodynamic performance of the unit is analyzed in detail. The numerical results demonstrate that the tip vortex plays a major role in the flow fields near the blade tip and has a great effect on the flow field of the unit. In addition, the inlet ring's size and throat's depth of the bell-mouth type shroud, and the through-flow area and configuration of upwind and downwind sections of the outlet grille are the most important factors that affect the aerodynamic performance of the outdoor unit.

(4) Two improved schemes against the existing prototype of unit are developed, which both can significantly increase the flow rate more than 6 % (i.e. 100 m^3 • h^{-1}) and are capable of delivering the same flow rate at lower rotating speeds. However the inevitable increase of flow noise in proportion to the increase of flow rate is demonstrated.

References

[1] WU C J, LIU D P, PAN J. A study of the aerodynamic and acoustic performance of an indoor unit of a DC-inverter split air-conditioner[J]. *Applied. Acoustics*, 2012, 73 (4): 415–422.

[2] JANG C M, FURUKAWA M, INOUE M. Analysis of vortical flow field in a propeller fan by LDV measurements and LES-Part I: Three-dimensional vortical flow structures[J]. *ASME Journal of Fluids Engineering*, 2001, 123 (4): 748–754.

[3] JANG C M, FURUKAWA M, INOUE M. Analysis of vortical flow field in a propeller fan by LDV measurements and LES-Part II: Unsteady nature of vortical flow structures due to tip vortex breakdown[J]. *ASME Journal of Fluids Engineering*, 2001, 123 (4): 755–761.

[4] KATO C, KAIHO M, MANABE A. An overset finite-element large-eddy simulation method with application to turbomachinery and aeroacoustic[J]. *ASME Journal of Applied Mechanics*, 2003, 70(1): 32–43.

[5] YAMADE Y, KATO C, SHIMIZU H. Large eddy simulation and acoustical analysis for prediction of aeroacoustics noise radiated from an axial-flow fan[C]//*Proceedings of ASME/FEDSM2006*, Miami, USA, July 17–20, 2006: 453–462.

[6] KATO C, YAMADE Y, WANG H, et al. Numerical prediction of sound generated from flows with a low Mach number[J]. *Computers & Fluids*, 2007, 36(1): 53–68.

[7] JIANG C L, TIAN J, OUYANG H, et al. Investigation of air-flow fields and aeroacoustic noise in outdoor unit for split-type air-conditioner[J]. *Noise Control Engineering Journal*, 2006, 54(3): 146–156.

[8] JIANG C L, CHEN J P, CHEN Z J, et al. Experimental and numerical study on aeroacoustic sound of axial flow fan in room air-conditioner[J]. *Applied. Acoustics*, 2007, 68(4): 458–472.

[9] HAMADA S, NAKASHIMA S, KATO C, et al. Aerodynamic noise simulation of propeller fan by large eddy simulation[C]// *Proceedings of 5th Joint ASME/JSME Fluids Engineering Conference*, San Diego, USA, July 30–August 2, 2007: 1–8.

[10] CAROLUS T, SCHNEIDER M, REESE H. Axial flow fan

broad-band noise and prediction[J]. *Journal of Sound and Vibration*, 2007, 300(1–2): 50–70.

[11] REESE H, CAROLUS T, KATO C. Numerical prediction of the aeroacoustic sound sources in a low pressure axial fan with inflow distortion[C]//*Proceedings of Fan Noise 2007*, Lyon, France, September 17–19, 2007: 1–12.

[12] ALGERMISSEN G, SIEGERT R, SPINDLER T. Numerical simulation of aeroacoustic sound generated by fans under installation conditions[C]//*7th AIAA/CEAS Aeroacoustics Conference*, Maastricht, Netherlands, May 28–30, 2001: 1–10 (AIAA Paper No. 2001–2174).

[13] NALLASAMY M, ENVIA E, THORP S A, et al. Fan noise source diagnostic test- computation of rotor wake turbulence noise[C]//*8th AIAA/CEAS Aeroacoustics Conference*, Breckenridge, USA, June 17–19, 2002: 1–13(AIAA Paper No. 2002–2489).

[14] MAALOUM A, KOUIDRI S, BAKIR F, et al. Effect of inlet duct contour and lack thereof on the noise generated of an axial flow fan[J]. *Applied Acoustics*, 2003, 64(10): 999–1010.

[15] HU J W, DING G L. Effect of the air outlet louver on the noise generated by the outdoor set of a split-unit air-conditioner[J]. *Applied Thermal Engineering*, 2006, 26(14–15): 1737–1745.

[16] HU J W, DING G L. Effect of deflecting ring on noise generated by outdoor set of a split-unit air-conditioner[J]. *International Journal of Refrigeration*, 2006, 29(3): 505–513.

[17] TIAN J, OUYANG H, WU Y D. Experimental and numerical study on aerodynamic noise of outdoor unit of room air-conditioner with different grilles[J]. *International Journal of Refrigeration*, 2009, 32(5): 1112–1122.

[18] WEI E P T, SHUKOR M H A. A study of effects of surrounding structures towards airflow performance in the outdoor unit of split-type air-conditioners[C]//*Proceedings of the 6th WSEAS International Conference on FLUID MECHANICS*, Ningbo, China, January 10–12, 2009: 15–21.

[19] HASE T, YAMASAKI N, OOISHI T. Numerical simulation for fan broadband noise prediction[J]. *Jounal of Thermal Science*, 2011, 20 (1): 58–63.

[20] MOON Y J, CHO Y, NAM H S. Computation of unsteady viscous flow and aeroacoustic noise of cross-flow fans[J]. *Computers & Fluids*, 2003, 32 (7): 995–1015.

[21] *FLUENT 6.3 user's guide*[EB/OL]. Fluent Inc., 2006[2012-12-10]. http://aerojet.engr.ucdavis.edu/fluenthelp/ html/ug/main_pre.htm.

Biographical notes

WU Chengjun, born in 1968, is currently a professor at *School of Mechanical Engineering*, *Xi'an Jiaotong University*, *China*. He received his PhD degree from *Xi'an Jiaotong University*, *China*, in 1999. His research interests include mechanical dynamics, CFD/CAA simulation, and damping technology application.
Tel: +86-29-82668573; E-mail: cjwu@mail.xjtu.edu.cn

LIU Jiang, born in 1986. He recievd his master degree from *Xi'an Jiaotong University*, *China*, in 2011. His research interests include vibration and noise control for mechanical structures, and CFD/CAA simulation.
E-mail: 414238313@qq.com

PAN Jie, born in 1957, is currently a professor at *Centre for Acoustics, Dynamics and Vibration*, *School of Mechanical and Chemical Engineering*, *The University of Western Australia*, *Australia*. He received his PhD degree from *The University of Adelaide*, *Australia*, in 1989. His research interests include mechanical dynamics, acoustics, vibration and noise control for mechanical structures, and CFD/CAA simulation.
E-mail: pan@mech.uwa.edu.au